Supporting Information

Caspase-3 Substrates for Non-Invasive Pharmacodynamic Imaging of Apoptosis by PET/CT.

Authors

Brian J. Engel[1], Seth T. Gammon[1], Rajan Chaudhari[2], Zhen Lu[2], Federica Pisaneschi[1], Hailing Yang[2], Argentina Ornelas[1], Victoria Yan[1], Lindsay Kelderhouse[1], Amer M. Najjar[3], William P. Tong[1], Shuxing Zhang[2,4], David Piwnica-Worms[1,5], Robert C. Bast Jr.[2], Steven W. Millward[1]*.

[1]Department of Cancer Systems Imaging, The University of Texas MD Anderson Cancer Center, 1515 Holcombe Blvd, Houston, TX 77030.

[2]Department of Experimental Therapeutics, The University of Texas MD Anderson Cancer Center, 1515 Holcombe Blvd, Houston, TX 77030.

[3]Department of Pediatrics - Research, The University of Texas MD Anderson Cancer Center, 1515 Holcombe Blvd, Houston, TX 77030.

[4]School of Biomedical Informatics, The University of Texas Health Science Center at Houston, Houston, TX 77030.

[5]Department of Cancer Biology, The University of Texas MD Anderson Cancer Center, 1515 Holcombe Blvd, Houston, TX 77030.

*Corresponding Author

Table of Contents

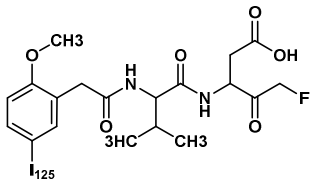

Figure S1: Structure of caspase inhibitor M808.

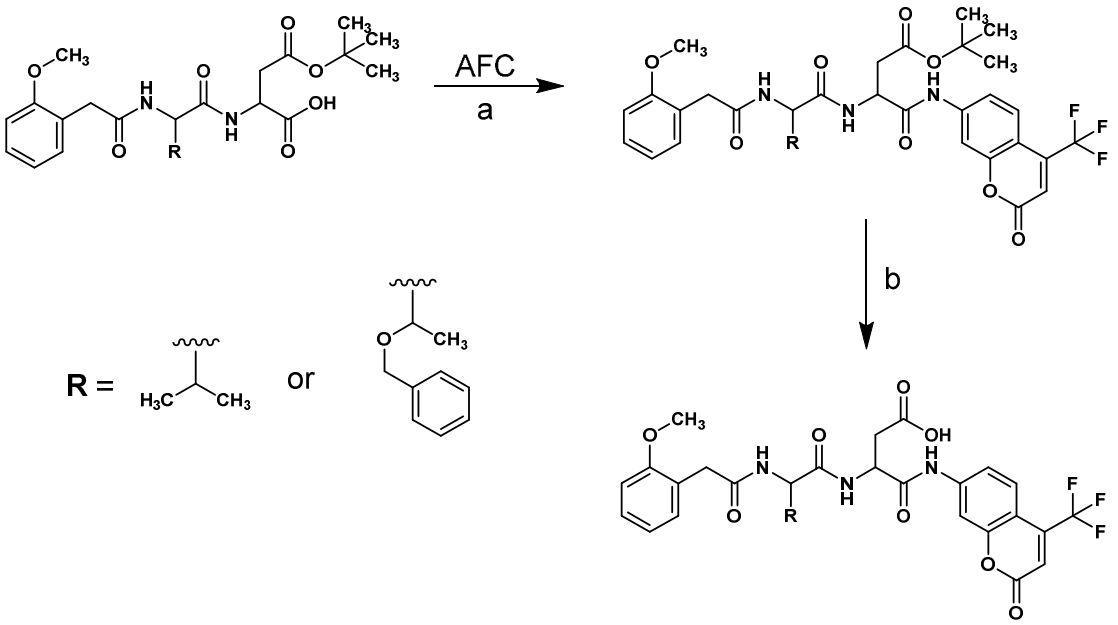

Scheme S1. Synthesis of fluorescent caspase-3 substrates. Reagents and conditions: (a) HATU, DIEA, DMF, 25 °C, 6 hrs; (b) 95:5 TFA:H_2O, 25 °C, 1 hr. AFC - 7-amino-4-(trifluoromethyl)coumarin.

Table S1: Kinetic parameters and product formation rates for 1, 2, and Ac-DEVD-AFC.

Substrate	Hydrolyzed Product (ng)	K_M (μM)	V_{max} (nmol/min)	k_{cat} (s^{-1})	k_{cat}/K_M ($\mu M^{-1}s^{-1}$)
1	1.2±0.2	264±61.4	0.014±0.001	$6.3 \times 10^{-5} \pm 4.5 \times 10^{-6}$	0.24
2	5.2±0.5	336±60.3	0.065±0.004	$2.9 \times 10^{-4} \pm 1.7 \times 10^{-5}$	0.87
Ac-DEVD-AFC	741.1±5.3	4.3±0.4	0.303±0.007	$5.9 \times 10^{-3} \pm 1.4 \times 10^{-4}$	1370

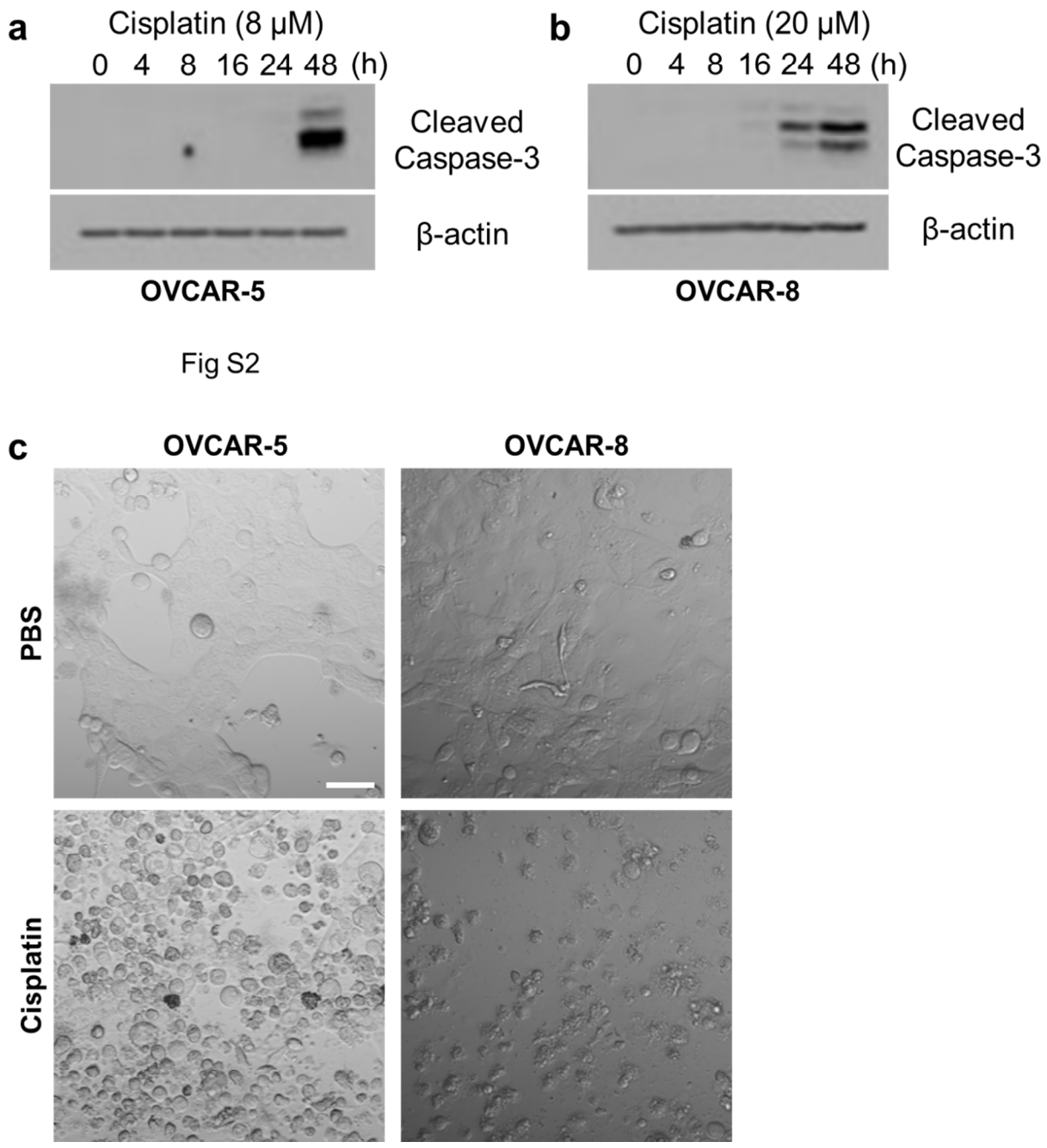

Figure S2. Confirmation of induction of apoptosis by cisplatin treatment. Western blot of **a**: OVCAR-5 and **b**: OVCAR-8 cells treated with 8 μM and 20 μM cisplatin, respectively, for 0-48 hours. **c**: Brightfield imaging of OVCAR-5 and OVCAR-8 cells treated with PBS or cisplatin for 48 hours. Cisplatin induces phenotypic apoptosis in cells. Scale bar represents 50 μm.

Table S2. Physicochemical properties of caspase-3 substrates. LogP calculated with ChemBioDraw v14.

Compound	LogP	MW	H-Bond Donors	H-Bond Acceptors
1	1.85	591.54	4	11
2	2.52	683.64	4	12
3	0.08	506.54	4	12
4	0.18	620.56	4	12
5	0.39	520.24	4	12
6	0.61	534.59	4	12
7	1.1	548.62	4	12
8	1.5	574.65	4	12
9	1.9	596.66	4	12
10	0.13	603.7	4	13
11	-1.07	563.59	5	14
12	-0.58	577.61	5	14
13	1.09	653.71	5	14
14	-1.43	593.61	6	15
15	0.85	612.66	4	13
16	0.75	598.63	4	13
17	1.01	612.66	3	13
18	1.53	554.62	3	11
19	2.35	660.27	4	13
20	2.35	660.27	4	13

Table S3: Kinetic parameters for caspase-3 hydrolysis of substrates 3 and 16.

Substrate	K_m (μM)	V_{max} (nmol/min)	k_{cat} (s^{-1})	k_{cat}/K_m ($\mu M^{-1}s^{-1}$)
3	2260±622	0.0012±0.00015	$4.5 \times 10^{-6} \pm 5.1 \times 10^{-7}$	0.0013
16	3190±1150	0.021±0.004	$7.1 \times 10^{-5} \pm 1.3 \times 10^{-5}$	0.022

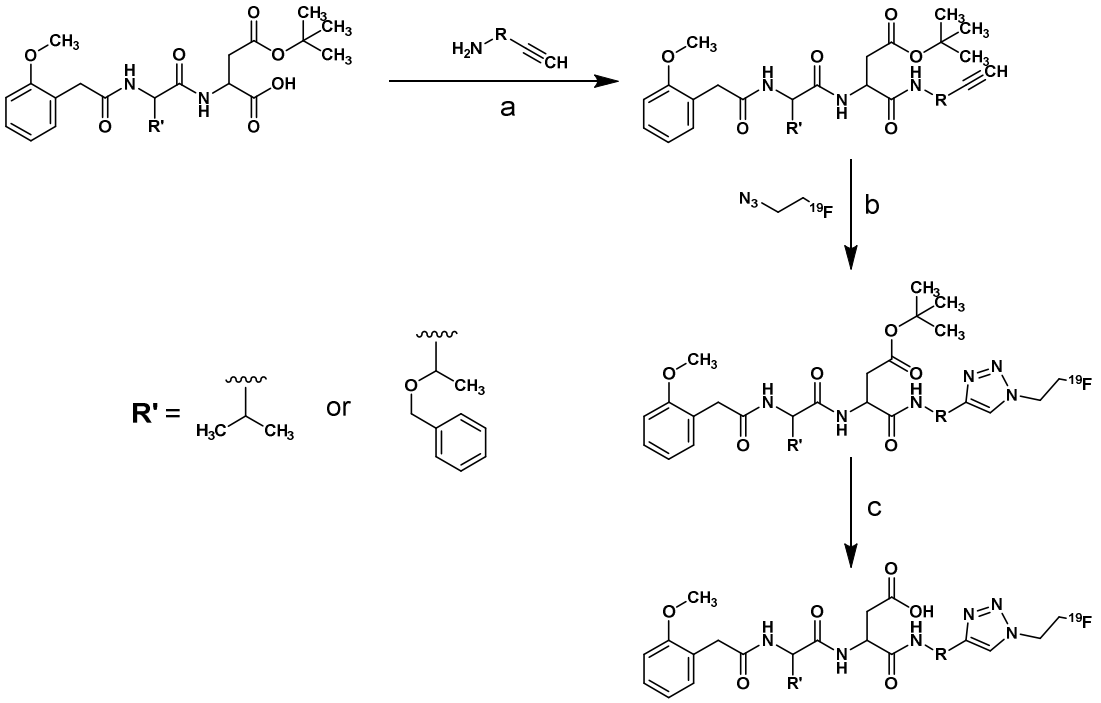

Scheme S2. Synthesis of cold radiotracer caspase-3 substrates. Reagents and conditions: (a) HBTU, DIEA, DMF, 25 °C, 6 hrs; (b) $CuSO_4$, L-ascorbic acid, 1:1 DMF:H_2O, 25 °C 16 hrs; (c) 95:5 TFA:H_2O, 25 °C, 1 hr. AFC - 7-amino-4-(trifluoromethyl)coumarin. Refer to Table 1 for **R** sidegroups.

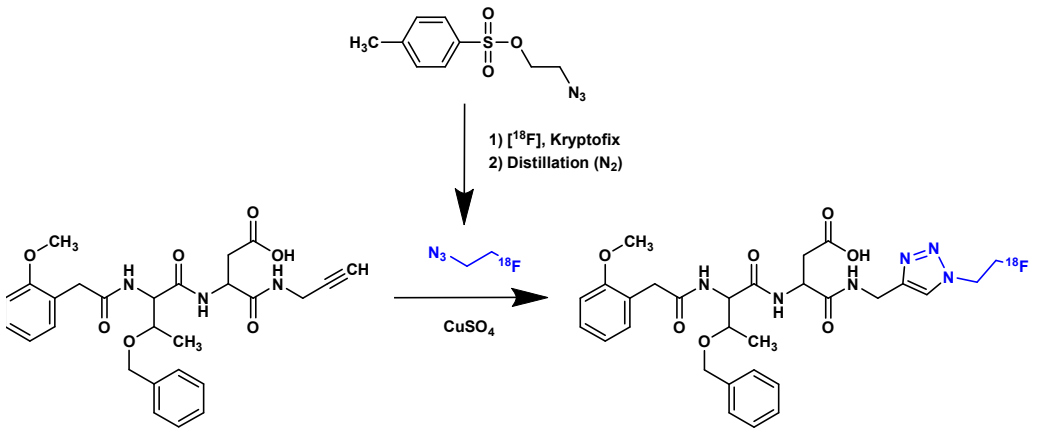

Scheme S3: Synthesis of [18F]-16 ([18F]-TBD). Alkyne precursor was conjugated to 2-[^{18}F]-fluoroethylazide *via* Cu-catalyzed azide-alkyne click chemistry with a GE Tracerlab to produce the fluorine-18-labeled product.

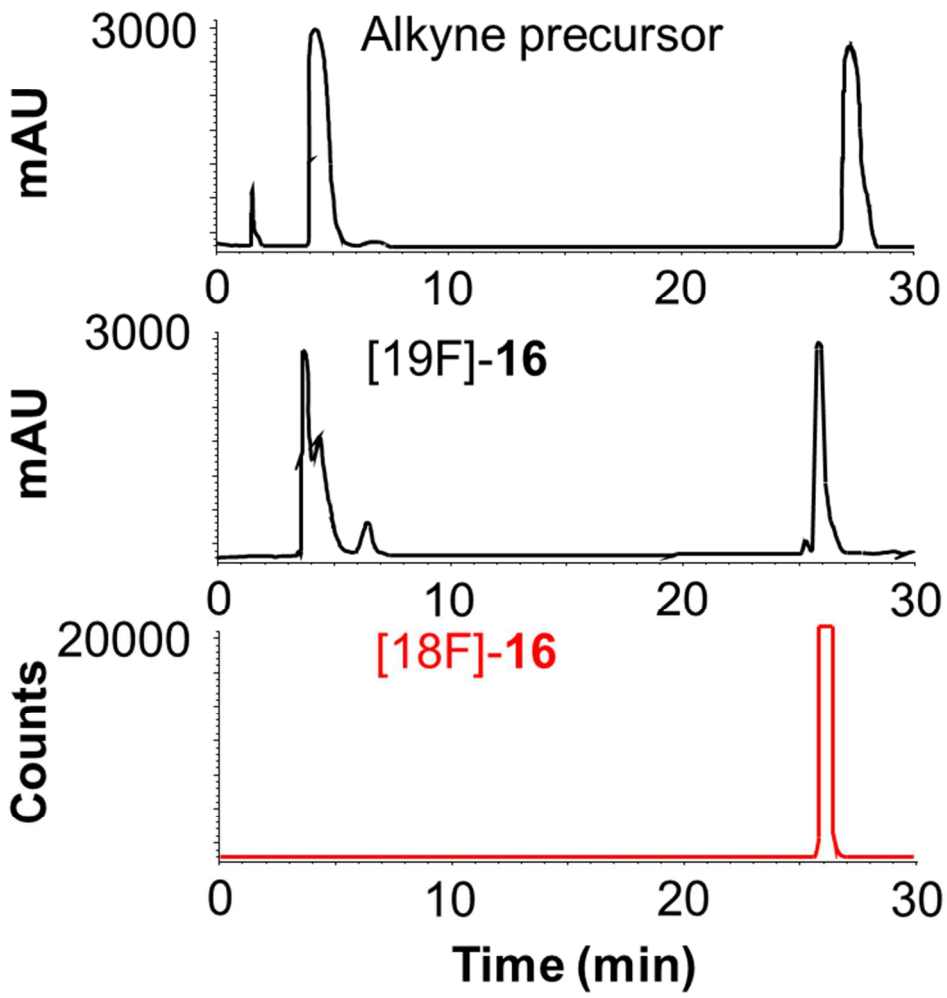

Figure S3. RadioHPLC analysis of [F18]-16. 20 µL of product was analyzed by radio-HPLC on a C18 column (Econosil C18, 10 µm, 250 mm, 4.6 mm), a water (0.1% (v/v) TFA) and CH_3CN (0.1% (v/v) TFA) gradient (5% B → 60% B in 30 min) with a flow of 1 mL/min.

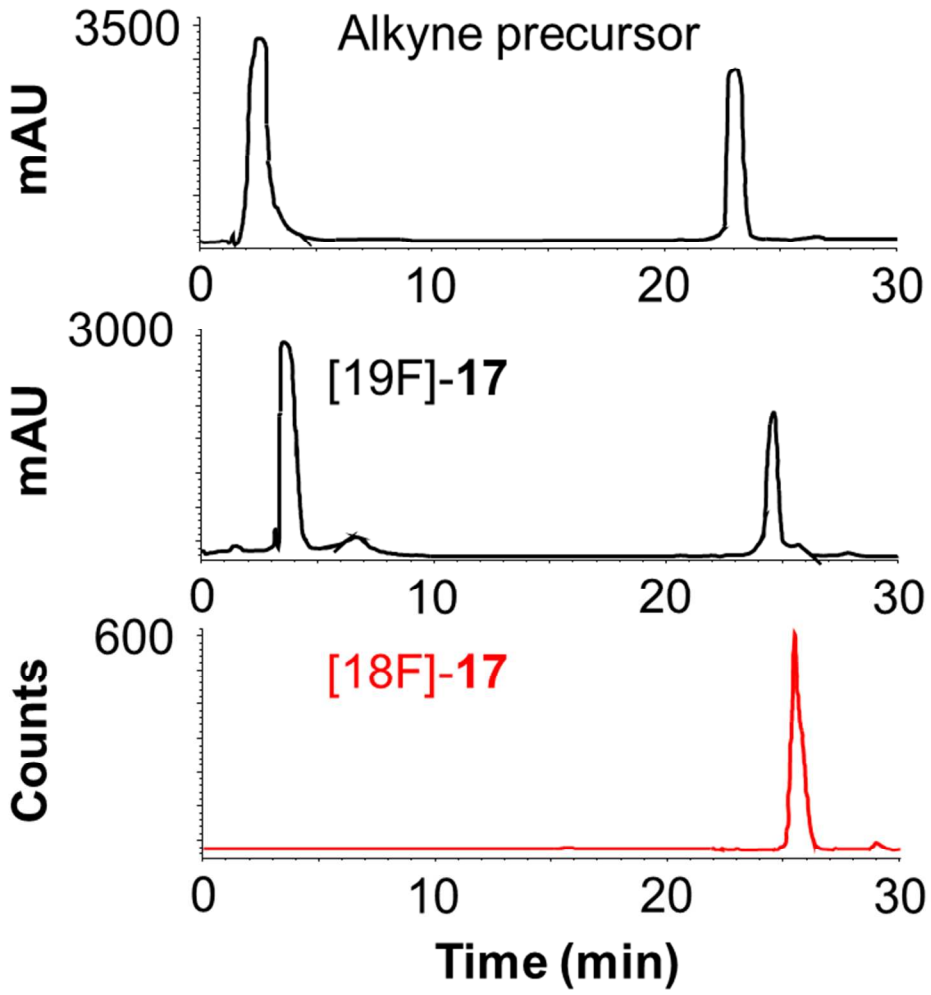

Figure S4. RadioHPLC analysis of [F18]-17. 20 µL of product was analyzed by radio-HPLC on a C18 column (Econosil C18, 10 µm, 250 mm, 4.6 mm), a water (0.1% (v/v) TFA) and CH_3CN (0.1% (v/v) TFA) gradient (5% B → 60% B in 30 min) with a flow of 1 mL/min.

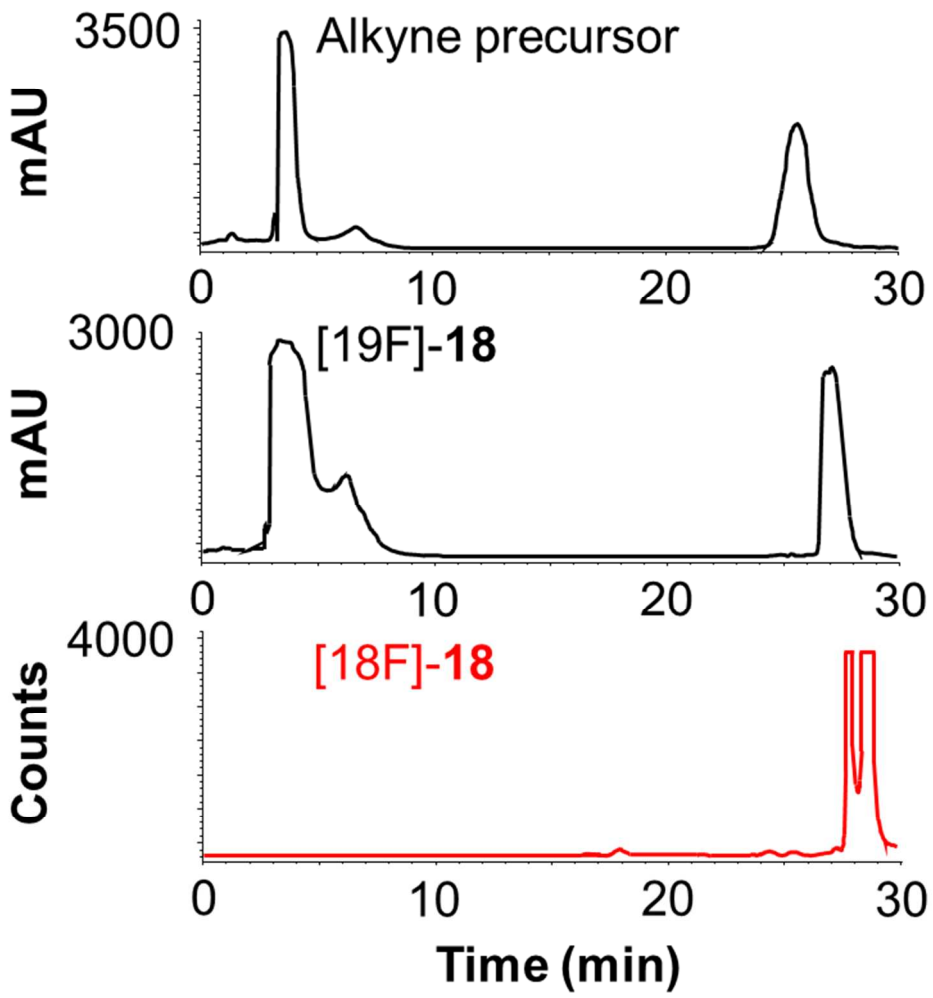

Figure S5. RadioHPLC analysis of [F18]-18. 20 µL of product was analyzed by radio-HPLC on a C18 column (Econosil C18, 10 µm, 250 mm, 4.6 mm), a water (0.1% (v/v) TFA) and CH_3CN (0.1% (v/v) TFA) gradient (5% B → 60% B in 30 min) with a flow of 1 mL/min.

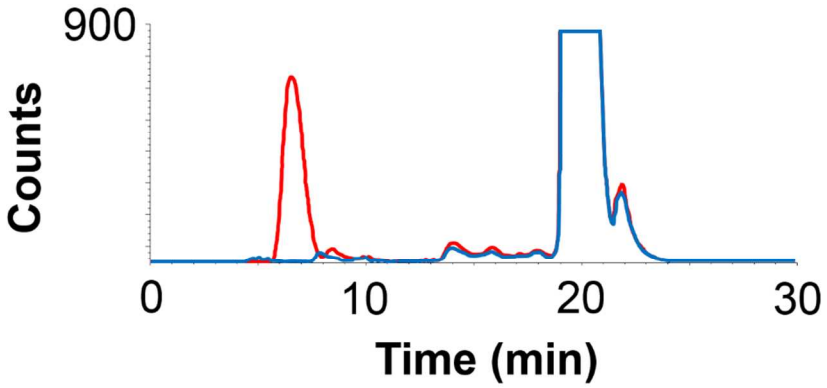

Figure S6. Radiotracer [18F]-16 is hydrolyzed in vitro by caspase-3. Radio HPLC trace of [18F]-**16** treated with caspase-3 (red) or a no caspase-3 control (blue). Hydrolyzed tracer had a retention time of 6.5 min versus 20 min for the intact probe.

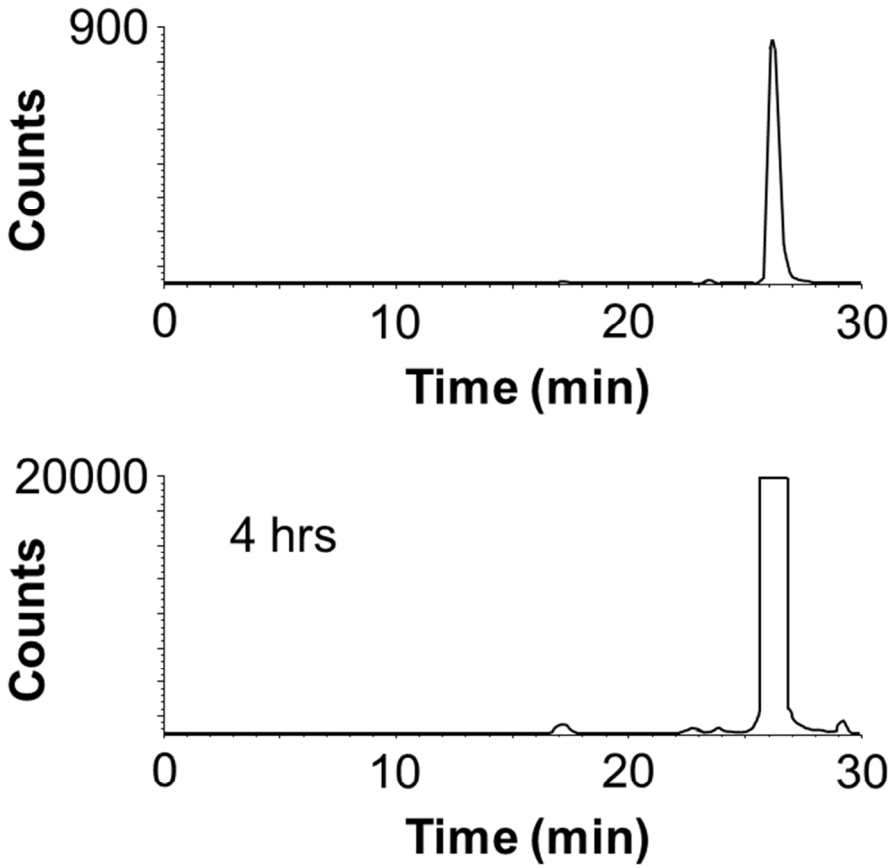

Figure S7. *In vitro* stability of [F18]-16. 20 µL of product was analyzed by radio-HPLC on a C18 column (Econosil C18, 10 µm, 250 mm, 4.6 mm), a water (0.1% (v/v) TFA) and CH_3CN (0.1% (v/v) TFA) gradient (5% B → 60% B in 30 min) with a flow of 1 mL/min immediately after elution with ethanol (top) or after 4 hours incubated at room temperature (bottom). Differences in counts are from increasing the sensitivity of the gamma detector to compensate for radioactive decay.

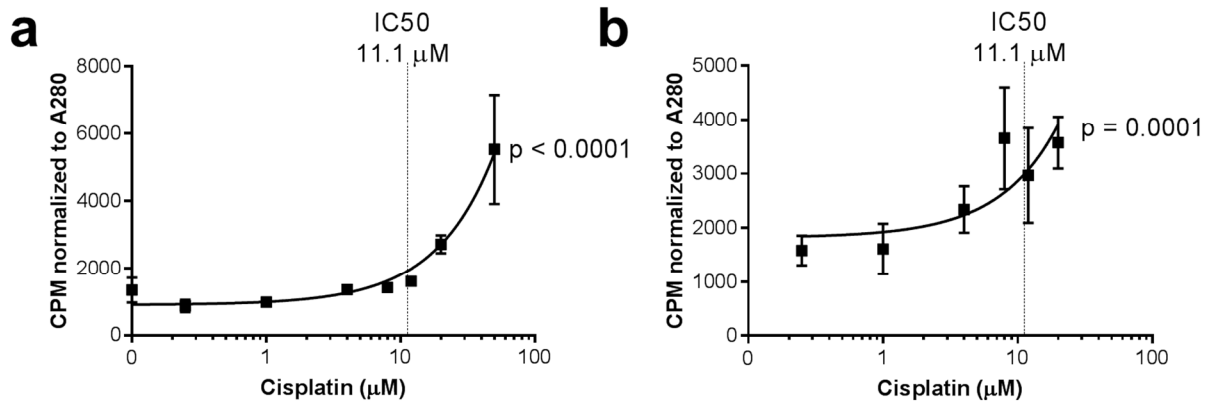

Figure S8. [18F]-16 accumulates in OVCAR8 cells treated with cisplatin. Accumulation of [18F]-**16** in OVCAR-8 cells treated with 0-50 μM cisplatin for 48 hours, then 5 μCi of [18F]-**16** for 1 hour and washed at 37 °C (**a**) or 4 °C (**b**). Reported IC50 indicated by dotted line[16]. Normalized gamma counts were graphed (means ± standard deviation) against cisplatin concentration and fit to a non-linear regression. Statistical F-test finds that the slope is non-zero with high certainty, n =3 for each condition.

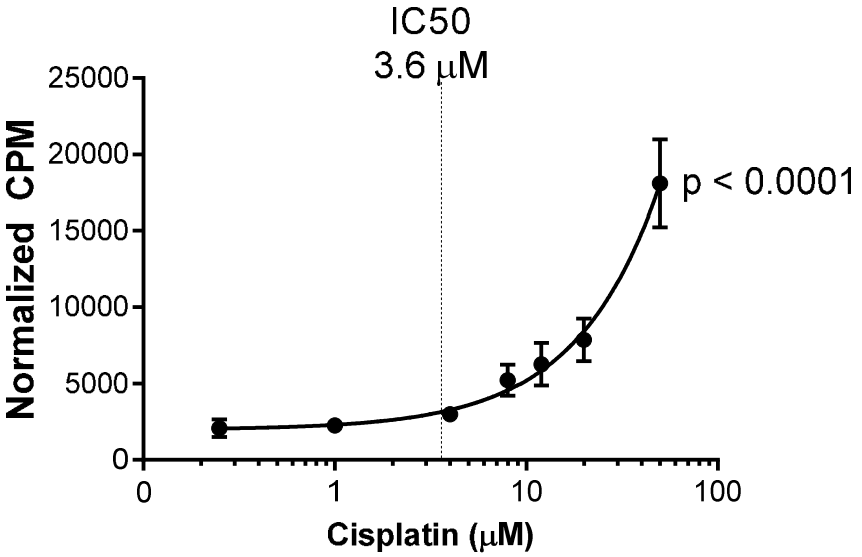

Figure S9. [18F]-16 accumulates in OVCAR5 cells treated with cisplatin and washed at 4 °C. Accumulation of [18F]-**16** in OVCAR-5 cells treated with 0-50 μM cisplatin for 48 hours, then 5 μCi of [18F]-**16** for 1 hour and washed at 4 °C. Reported IC50 indicated by dotted line[16]. Normalized gamma counts were graphed (means ± standard deviation) against cisplatin concentration and fit to a non-linear regression. Statistical F-test finds that the slope is non-zero with high certainty.

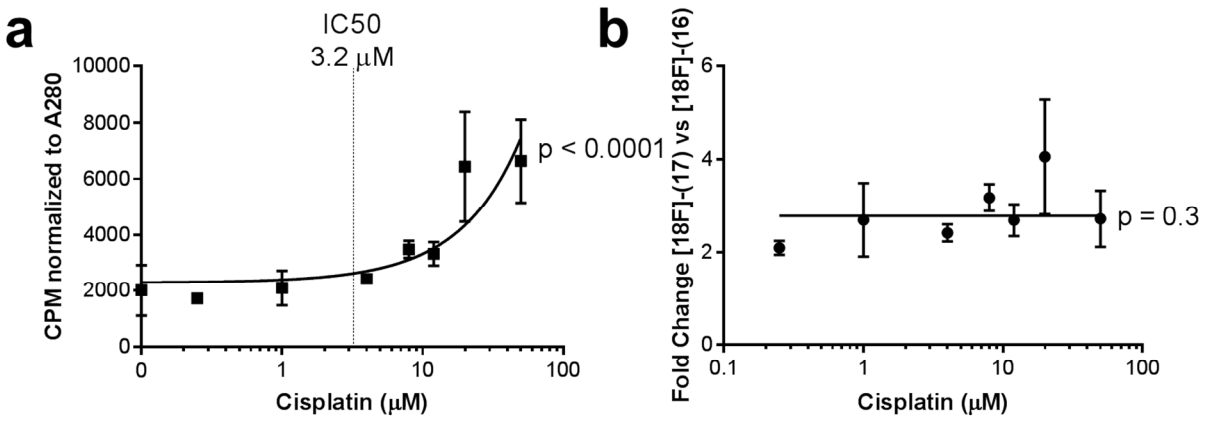

Figure S10. Methyl protection of aspartic acid doubles probe accumulation. a: OVCAR-5 cells were treated with 0-50 μM cisplatin for 48 hours and then 5 μCi of [18F]-**17** for 1 hour. Reported IC50 indicated by dotted line[16]. Normalized gamma counts were graphed (means ± standard deviation) against cisplatin concentration and fit to a non-linear regression. **b**: Comparison of cisplatin dependent accumulation of [18F]-**17** vs [18F]-**16** in OVCAR5 cells. Accumulation is independent of cisplatin concentration. Statistical F-test finds that the slope is non-zero with high certainty in **a** and not significant in **b**, n = 3 for each condition.

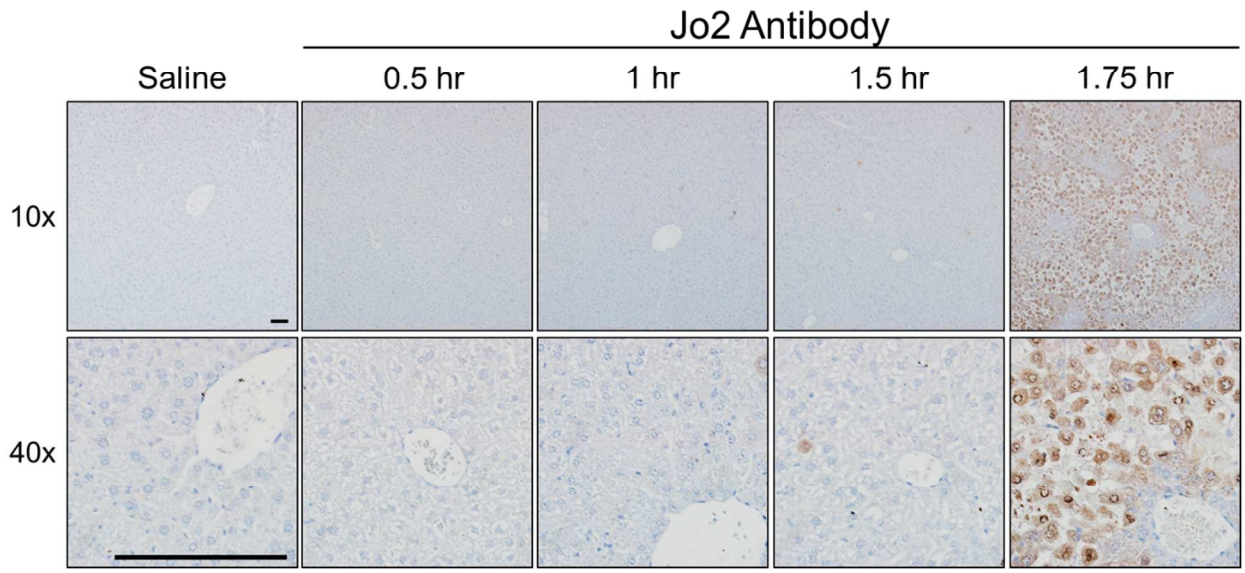

Figure S11. Cleaved caspase-3 staining in Jo2-treated mouse liver. Mice were treated with saline or 10 µg Jo2 antibody *i.v*. After the times listed, animals were sacrificed and livers fixed and stained for cleaved caspase-3. Scale bar represents 200 µm.

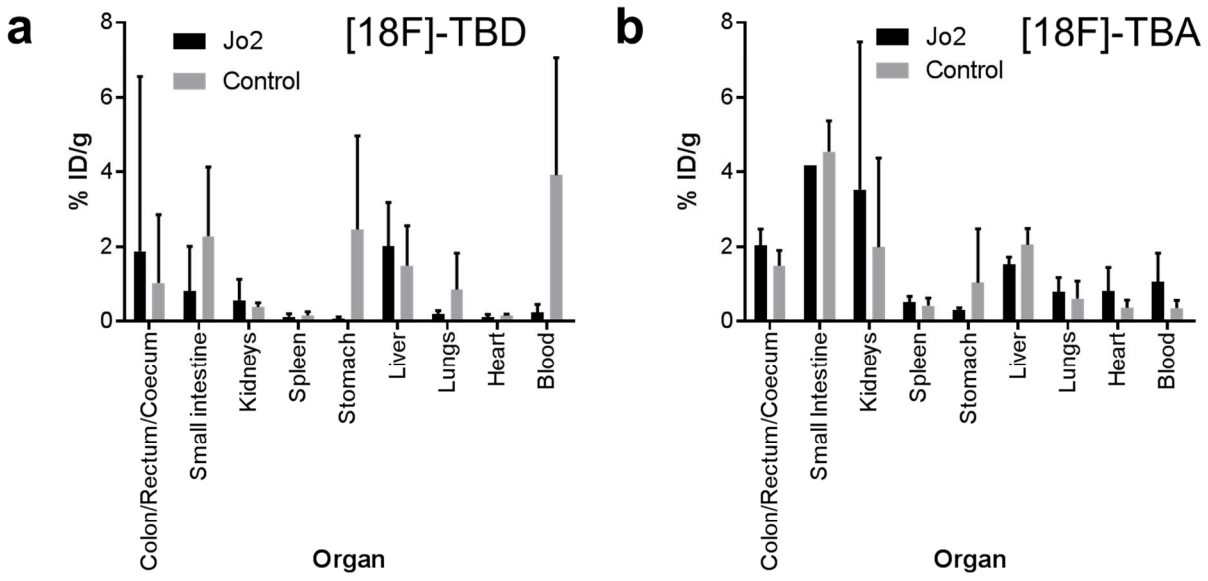

Figure S12. Biodistribution of F18-labeled probes. Mice were anesthetized, injected i.v. with [18F]-TBD (**a**) or [18F]-TBA (**b**) and then subjected to a 30 min dynamic PET with 5 min CT. Immediately after, mice were euthanized and organs harvested and radioactivity measured with a gamma counter. Organs were weighed and percent of injected dose per gram tissue calculated. Bars represent means ± standard deviation. n = 7 ([18F]-TBD Jo2), n = 4 ([18F]-TBD control), n = 2 ([18F]-TBA Jo2), n = 3 ([18F]-TBA control).

Table S4. Summary of kinetic parameters from of dynamic PET modeling.

		k1 (1/sec)				k2 (1/sec)				k3 (1/sec)			
Probe	**Treatment**	**Estimate**	**Standard Error**	**T-Statistic**	**P-Value**	**Estimate**	**Standard Error**	**T-Statistic**	**P-Value**	**Estimate**	**Standard Error**	**T-Statistic**	**P-Value**
16	Control	1.98E-02	4.98E-03	3.97	3.65E-04	1.89E-12	1.31E-03	1.44E-09	1	1.78E-03	3.67E-04	4.84	2.94E-05
16	Control	1.55E-02	2.21E-03	7.02	1.51E-09	5.86E-13	5.69E-04	1.03E-09	1	1.20E-03	1.23E-04	9.72	2.32E-14
16	Control	5.14E-03	7.54E-04	6.83	3.30E-09	5.86E-13	9.30E-04	6.30E-10	1	1.46E-03	5.78E-04	2.53	1.37E-02
16	Control	1.21E-02	1.68E-03	7.25	5.82E-10	5.86E-13	7.61E-04	7.71E-10	1	1.81E-03	1.98E-04	9.18	2.08E-13
16	Jo2	1.69E-02	1.53E-03	11.00	1.34E-12	5.86E-13	2.31E-04	2.54E-09	1	6.30E-04	9.83E-05	6.41	2.93E-07
16	Jo2	4.33E-02	5.87E-03	7.38	3.35E-10	3.81E-12	3.17E-04	1.20E-08	1	7.58E-04	1.01E-04	7.52	1.92E-10
16	Jo2	4.09E-02	8.08E-03	5.06	3.53E-06	3.48E-12	7.37E-04	4.72E-09	1	1.80E-03	2.49E-04	7.26	5.68E-10
16	Jo2	1.14E-02	1.41E-03	8.11	2.27E-11	7.70E-12	8.08E-04	7.26E-10	1	1.05E-03	1.08E-04	15.86	1.13E-23
16	Jo2	2.60E-02	4.10E-03	6.33	2.42E-08	5.86E-13	4.86E-04	1.21E-09	1	1.03E-03	1.58E-04	6.56	9.67E-09
16	Jo2	2.74E-02	4.52E-03	6.05	7.49E-08	5.86E-13	4.69E-04	1.25E-09	1	7.82E-04	2.59E-04	3.02	3.55E-03
16	Jo2	4.96E-02	9.12E-03	5.44	8.42E-07	5.86E-13	3.37E-04	1.74E-09	1	7.34E-04	9.90E-05	7.41	2.98E-10
18	Control	3.85E-02	8.10E-03	4.75	1.13E-05	5.86E-13	5.55E-04	1.06E-09	1	8.95E-04	2.53E-04	3.54	7.38E-04
18	Control	2.09E-02	3.46E-03	6.05	7.49E-08	5.86E-13	4.80E-04	1.22E-09	1	8.34E-04	2.65E-04	3.15	2.45E-03
18	Control	3.58E-02	1.00E-02	3.57	6.75E-04	5.86E-13	9.37E-04	6.26E-10	1	1.50E-03	3.61E-04	4.14	9.92E-05
18	Jo2	3.22E-03	6.79E-04	4.74	1.19E-05	5.86E-13	1.34E-03	4.37E-10	1	6.48E-04	1.10E-03	0.59	5.57E-01
18	Jo2	1.18E-02	2.00E-03	5.88	1.51E-07	5.86E-13	8.71E-04	6.73E-10	1	1.42E-03	4.10E-04	3.47	9.18E-04

		k4 (1/sec)				k5 (1/sec)				k6 (1/sec)			
Probe	**Treatment**	**Estimate**	**Standard Error**	**T-Statistic**	**P-Value**	**Estimate**	**Standard Error**	**T-Statistic**	**P-Value**	**Estimate**	**Standard Error**	**T-Statistic**	**P-Value**
16	Control	1.42E-11	8.47E-04	1.68E-08	1	2.37E-02	6.90E-03	3.43	1.65E-03	1.22E-12	3.32E-04	3.67E-09	1
16	Control	5.86E-13	3.04E-04	1.93E-09	1	1.30E-02	2.32E-03	5.60	4.51E-07	5.86E-13	1.51E-04	3.87E-09	1
16	Control	1.46E-03	4.41E-04	3.30	1.54E-03	1.18E-02	1.68E-03	7.04	1.36E-09	5.86E-13	2.84E-04	2.07E-09	1
16	Control	5.86E-13	3.60E-04	1.63E-09	1	1.03E-02	1.78E-03	5.78	2.23E-07	5.86E-13	1.53E-04	3.83E-09	1
16	Jo2	1.20E-03	2.06E-04	5.85	1.49E-06	2.85E-02	2.63E-03	10.83	2.01E-12	7.43E-04	2.40E-04	3.09	4.06E-03
16	Jo2	2.04E-03	6.66E-04	3.07	3.14E-03	6.86E-02	9.31E-03	7.37	3.52E-10	5.45E-04	2.14E-04	2.55	1.31E-02
16	Jo2	1.79E-04	1.48E-03	0.12	0.90	7.44E-02	1.45E-02	5.15	2.57E-06	7.75E-05	2.07E-04	0.37	0.71
16	Jo2	5.86E-13	2.10E-04	2.79E-09	1	1.52E-03	6.94E-04	2.19	3.19E-02	1.59E-04	7.59E-05	7.72E-09	1
16	Jo2	5.86E-13	7.25E-04	8.09E-10	1	3.47E-02	5.71E-03	6.08	6.68E-08	5.86E-13	1.99E-04	2.95E-09	1
16	Jo2	5.13E-03	1.28E-03	4.02	1.53E-04	3.64E-02	6.44E-03	5.65	3.73E-07	5.86E-13	2.55E-04	2.30E-09	1
16	Jo2	6.10E-04	8.84E-04	0.69	0.49	7.96E-02	1.49E-02	5.36	1.15E-06	5.86E-13	1.74E-04	3.36E-09	1
18	Control	3.83E-03	1.69E-03	2.27	2.66E-02	9.91E-02	2.01E-02	4.93	5.85E-06	3.21E-12	2.88E-04	1.11E-08	1
18	Control	2.90E-03	9.70E-04	2.99	3.90E-03	4.60E-02	7.52E-03	6.12	5.81E-08	5.86E-13	2.78E-04	2.11E-09	1
18	Control	2.99E-03	2.01E-03	1.49	0.14	1.40E-01	3.46E-02	4.04	1.44E-04	5.86E-13	2.99E-04	1.96E-09	1
18	Jo2	2.16E-03	4.48E-04	4.83	8.51E-06	2.13E-02	2.76E-03	7.73	7.90E-11	5.86E-13	6.85E-04	8.56E-10	1
18	Jo2	2.09E-03	7.27E-04	2.88	5.42E-03	2.90E-02	4.08E-03	7.10	1.06E-09	5.86E-13	2.69E-04	2.18E-09	1